JSST
Journal of Space Science and Technology

P-ISSN: 2008-4560
E-ISSN: 2423-4516

Journal of Space Science and Technology

Vol. 17, Special Issue, pp. 22-31, 2024
https://doi.org/10.22034/jsst.2024.1491
Journal Homepage: https://jsstpub.com

Original Research Paper

Design and Analysis of Plasma-Based Reconfigurable Maxwell Fish Eye Lens Antennas

Jafar Bazrafshan[1], Fatemeh Sadeghikia[2*], Mohamed Himdi [3], Ali Karami Horestani[4], and Hajar Binti Ja'afar[5]

1, 2, 4. Aerospace Research Institute, Ministry of Science, Research and Technology, Tehran, Iran
3. University of Rennes 1, Rennes, France
5. School of Electrical Engineering, College of Engineering, MARA Technological University, Malaysia

ARTICLE INFO

Article History:

Received 09 July 2024
Revised 09 October 2024
Accepted 24 November 2024
Available Online 01 December 2024

Keywords:

Maxwell fish eye (MFE) lens
Plasma dielectric material
Reconfigurable antennas
Plasma lens antenna
Reconfigurable lens
Spherical lens
Hemispherical lens

ABSTRACT

This paper investigates the feasibility of employing plasma dielectric material to develop a Maxwell Fish Eye (MFE) lens antenna, functioning as a gradient index (GRIN) lens antenna with reconfigurability. The study focuses on the design, simulation, and analysis of both spherical and hemispherical MFE plasma lenses. Using geometric optics (GO), the analytical design equations of the Maxwell Fish Eye (MFE) lens are derived. Furthermore, the refractive index profile in the radial direction of the plasma-based MFE lens is extracted using the hyperbolic function—a conventional method for MFE lenses—while accounting for the unique property of plasma dielectrics, where the refractive index is smaller than 1. A prototype of the plasma-based MFE lens is designed based on the derived equations at an operating frequency of 10 GHz, and its performance is evaluated through numerical simulations considering a layered refractive index profile for the lens. The results reveal significant improvements in radiation characteristics, with the spherical configuration achieving a 6.5 dBi gain enhancement and the hemispherical lens demonstrating a remarkable 12.8 dBi gain enhancement. Additionally, the lens provides dynamic control over radiation patterns by leveraging the tunable nature of plasma. This reconfigurability is achieved by selectively switching plasma layers ON or OFF, effectively altering the lens's refractive index distribution in real time. Moreover, based on the results of a parametric analysis, a layer thickness of t = R/10, where R is the radius of the lens, provides the best trade-off between gain enhancement and implementation simplicity. The findings demonstrate the potential of plasma-based MFE lenses to achieve advanced reconfigurability in antenna systems. Such structures offer significant advantages for modern communication systems, where adaptability and beam shaping are critical. This work establishes a foundation for future research into plasma-enabled gradient index devices for reconfigurable antenna applications in 5G, 6G, and beyond.

*Corresponding Author's E-mail: sadeghi_kia@ari.ac.ir

How to Cite this Article:
J. Bazrafshan, F. Sadeghikia, M. Himdi, A. Karami Horestani, and H. Binti Ja'afar, "Design and analysis of plasma-based reconfigurable maxwell fish eye lens antennas," *Journal of Space Science and Technology*, Vol. 17, Special Issue, pp. 22-31, 2024, https://doi.org/10.22034/jsst.2024.1491.

1. INTRODUCTION

Microwave lenses are broadly classified into two categories based on their material composition: homogeneous and non-homogeneous. While homogeneous lenses are favorable due to their simple implementation [1], inhomogeneous lenses have garnered significant attention due to features such as high gain [2], the ability to generate multiple beams [3], controllable beam direction [4], and broadband radiation characteristics [5].

Among non-homogeneous lenses, the Maxwell fish-eye (MFE) lenses with spherical or hemispherical configurations, can direct electromagnetic waves to focus radiation from a wide field of view onto a focal point. Classified as a gradient index (GRIN) lens, the refractive index of the MFE lens changes smoothly from the center toward the outer layers [6-8].

The significance of MFE lenses in antenna design lies in their potential to enhance beamforming capabilities [9], improve long-range communication [5], and enable novel antenna configurations for diverse applications [10-14]. For instance, innovative designs such as multichannel lenses with beam splitters based on the MFE lens have been proposed in [10] and [11]. Moreover, using a combination of etched planar meta-surfaces and half MFE lens antennas, good focusing has been achieved [13]. In [14], wide-angle beam scanning has been demonstrated with MFE and Gutman lenses.

Driven by the need for adaptability and versatility in modern communication systems, reconfigurable antennas have become another essential concept in the field of antenna engineering [15]. Traditional approaches often face challenges in balancing performance and flexibility, relying on switching mechanisms that compromise efficiency and design simplicity [16]. Notable innovations have emerged, including optical methods using photoconductive materials, structural alterations in antenna configurations, and the incorporation of novel materials such as ferrite and plasmas into antenna structures.

Dynamic adjustment of plasma properties to create reconfigurable antennas has been investigated in various studies [17-30]. Demostrated antennas offer the advantage of adaptability, allowing for the dynamic tailoring of radiation patterns and beam directions without the need for complex switching components [31-36]. Traditional approaches to reconfiguring MFE lenses often rely on mechanical adjustments [10,12], and [14], such as sliding or rotating the lens or repositioning the feed source. While these methods provide beam control, they lack the rapid adaptability demanded by modern communication systems. These mechanical techniques, though effective, can be slow, bulky, and less precise for rapid real-time applications. In contrast, reconfigurable materials such as plasma offer a more dynamic solution, enabling real-time modifications to the refractive index by controlling plasma properties. This allows faster beam steering, and improved precision, and leads to the way for advanced features such as adaptive beamforming.

Although many studies have been carried out on the application of plasma media in their conductive mode for instance for the realization of antennas and reflectors [19-30], there are limited studies on the applications of plasma media in their dielectric mode, especially as dielectric lens antennas [17-19]. However, it is widely acknowledged that plasma structures exhibit favorable dielectric properties at frequencies higher than the plasma frequency. At such frequencies, control over the plasma refractive index can be achieved by adjusting the plasma frequency, presenting an opportunity for the development of dielectric lenses with controllable focal lengths [17].

This study explores the integration of plasma in its dielectric mode into an MFE lens, introducing a novel reconfigurable antenna system. While MFE lenses have been extensively studied both theoretically and experimentally, designing MFE lenses made of a dielectric with a refractive index of less than one represents a new frontier. To this end, existing analytical design equations for MFE lenses need to be modified, and the refractive index distribution profile must be redefined. Therefore, a key novelty of this research is the development of updated analytical design equations for MFE lenses incorporating plasma dielectrics, addressing a significant gap in the field.

Additionally, by controlling the refractive index of plasma, the lens characteristics can be dynamically adjusted, offering a more adaptable solution compared to traditional lenses. This reconfigurability, achieved by switching the lens layers ON or OFF, represents a second major novelty of this study. This paper aims to investigate

the feasibility of realizing this plasma-based lens and evaluating its performance.

The rest of the paper is organized as follows: Background information on plasma material in the dielectric mode is provided first. Next, the analytical design equations for spherical MFE lenses based on geometrical optics are presented. Then, the structure and design equations of MFE lenses based on plasma material are outlined. The performance of the proposed lens antenna is numerically analyzed in the subsequent section, followed by a detailed discussion and analysis of the findings. Finally, the study is concluded with insights into the significance of this research.

2. PLASMA DIELECTRIC THEORY

Plasma, in its general form, constitutes an ionized inert gas confined within a dielectric container. In this study, the dielectric mode of plasma material is used in the structure of the MFE lens, i.e., the plasma frequency is smaller than the operating frequency of the antenna [17]. The plasma medium is commonly represented using the Drude or Lorentz dispersion model, and under low-pressure conditions, its complex relative permittivity is defined as [37]:

$$\epsilon_p = 1 - \frac{\omega_p^2}{\omega(\omega - j\nu)} = \epsilon' + j\epsilon'', \tag{1}$$

Where ω = 2πf is the operating angular frequency, υ is the collision frequency of the plasma, and ωp = 2πfp is the plasma angular frequency. The plasma angular frequency is defined as:

$$\omega_p = \sqrt{Ne^2/m\varepsilon_0}, \tag{2}$$

Where m and e represent the electron mass and charge, N is the plasma electron density, and ε_0 denoted the free space permittivity. Neglecting the imaginary part of the plasma permittivity, the plasma relative permittivity is expressed as:

$$\varepsilon_p = 1 - \frac{\omega_p^2}{\omega^2 + \nu^2}. \tag{3}$$

The refractive index of plasma can be calculated based on the plasma permittivity:

$$n_p = \sqrt{\varepsilon_p} \tag{4}$$

It is important to note that, unlike conventional dielectrics, the plasma permittivity in plasma dielectrics, and consequently the refractive index of plasma, are smaller than one and greater than zero. Therefore, the phase velocity of an electromagnetic (EM) wave propagating in a plasma dielectric is higher than in free space. This characteristic significantly impacts the shape or distribution of the refractive index in lenses made of plasma [17].

3. ANALYTICAL DESIGN EQUATIONS

In this section, the analytical design equations and fundamental principles of spherical MFE plasma lenses are derived using the geometric optics (GO) method. These equations will be applied in the next section to design a prototype of a plasma-based MFE lens.

Let's start by analyzing the refractive index profile in MFE lenses, which plays a critical role in directing electromagnetic waves to achieve the desired focusing properties. A common mathematical model used to describe this profile for conventional MFE lenses is the hyperbolic function as follows [9]:

$$n(r) = \frac{n_0}{1+\left(\frac{r}{R}\right)^2} \qquad 0 < r < R \tag{5}$$

In this equation, n_0 represents the refractive index at the center of the sphere, R is the radius of the lens, and r is the radial distance from the center. This equation provides a smooth decrease in the refractive index from the center to the outer layers of the lens. By adjusting the parameters n_0 and R, it becomes possible to tailor the behavior of the lens antenna system.

In the geometric optics method [38], the Eikonal equation is a simplified form of the Maxwell's equations. It provides an approximation for describing the trajectory of rays in a medium with a spatially varying refractive index, such as MFE lens. The equation is given by [39]:

$$|\nabla u(\vec{r})| = n^2(\vec{r}) \tag{6}$$

where $\vec{r}$ is the radius vector, and $n(\vec{r})$ represents the refractive index of the medium. In two dimensions (on the x-y plane), the Eikonal equation becomes:

$$\left(\frac{\partial u(x,y)}{\partial x}\right)^2 + \left(\frac{\partial u(x,y)}{\partial y}\right)^2 = n^2(x,y) \tag{7}$$

Using the method of characteristics, this equation can be transformed into a system of ordinary differential equations (ODEs):

$$\begin{cases} \frac{dx}{dt} = \frac{p_1}{n^2} \\ \frac{dy}{dt} = \frac{p_2}{n^2} \\ \frac{dp_1}{dt} = \frac{1}{n}\frac{\partial n}{\partial x} \\ \frac{dp_2}{dt} = \frac{1}{n}\frac{\partial n}{\partial y} \end{cases} \quad (8)$$

where $p_1 = \frac{\partial u}{\partial x}$ and $p_2 = \frac{\partial u}{\partial y}$. The functions *x(t)*, *y(t)*, $p_1(t)$ and $p_2(t)$ describe the ray trajectories in the system. The partial derivatives of the refractive index, given by equation (5), in the *x*-*y* plane are expressed as follows.

$$\frac{\partial n(x,y)}{\partial x} = -\frac{2n^2(x,y)}{n_0 R^2}(x - X_0) \quad (9a)$$

$$\frac{\partial n(x,y)}{\partial y} = -\frac{2n^2(x,y)}{n_0 R^2}(y - Y_0) \quad (9b)$$

The initial conditions at $t = 0$ are defined by:

$$\begin{cases} x(t) = x_0 \\ y(t) = y_0 \\ p_1(t) = cos(\alpha)\, n(x_0, y_0) \\ p_2(t) = sin(\alpha)\ n(x_0, y_0) \end{cases} \quad (10)$$

Where α is the incident angle of the beam from the feed, and (x0, y0) represents the coordinates of the feed.

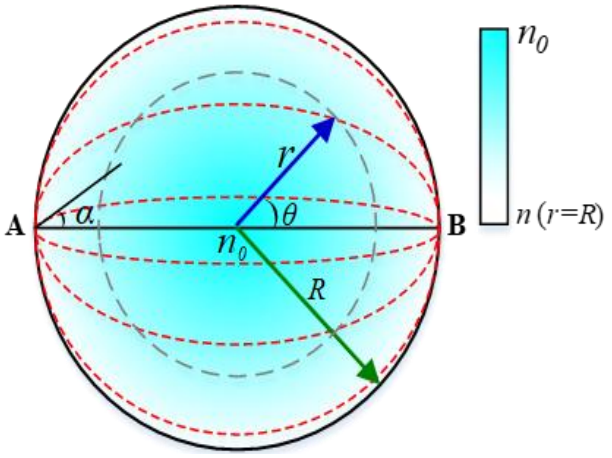

Fig. 1. Rays in a plasma-based MFE lens, with the representation of refractive index profile along the radial direction.

It's worth noting that the spherical MFE lens images a point on its surface to the opposite point, achieving diametric coverage, as illustrated in Fig. 1. The trajectory of a ray leaving point A and arriving at point B, diametrically opposite to point A, as depicted by the red dashed line in Fig. 1, is governed by the following equation [9]:

$$\theta = sin^{-1}\left(\frac{C(R^2 - r^2)}{Rr\sqrt{n_0^2 R^2 - 4C^2}}\right) \quad (11)$$

Here, *C* is a parameter that is constant for each layer, contributing to the trajectory of the ray within the lens structure.

It is noteworthy that the refractive index profile of a typical MFE lens using conventional dielectrics commonly ranges from $n_0 = 2$ at its center to $n = 1$ at the outer surface. However, since the refractive index of a plasma dielectric is always smaller than 1, it raises the question of whether it's feasible to use this type of dielectric in the MFE lens or not.

To address this, incorporating equations (3) and (5), and considering $n_0 = 1$, which represents the maximum refractive index of the plasma dielectric at the center of the lens, a design equation is extracted for the plasma MFE lens. Thus, the plasma frequency distribution profile for this lens is extracted as:

$$f_p(r) = \frac{1}{2\pi}\sqrt{(\omega^2 + \nu^2)\left(1 - \left(\frac{n_0}{1 + \left(\frac{r}{R}\right)^2}\right)^2\right)} \quad (12)$$

Using (12), it is possible to calculate the plasma frequency in different radii of a plasma MFE lens. To have a better insight into the differences between the refractive index profiles of a conventional MFE lens and the proposed plasma-based MFE lens, these two profiles are compared in Fig. 2, where both spherical lenses have a radius of $R = 100$ mm. It is evident from the figure that the range of variation in the refractive indices for the two lenses is significantly different. Additionally, while the refractive index profile in the plasma MFE lens is dependent on the operating frequency, it remains constant in the conventional MFE lens.

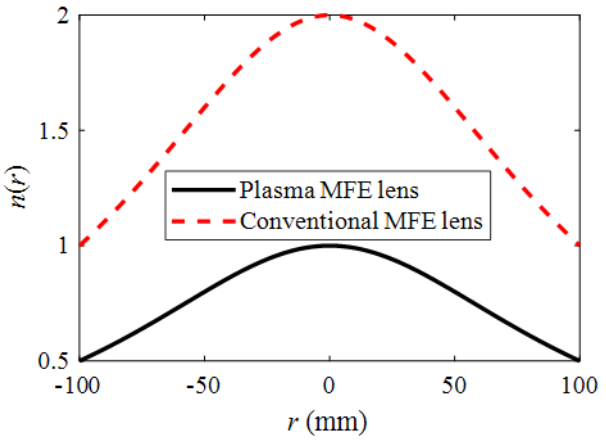

Fig. 2. Comparison of refractive index profile distributions along the radius of a conventional MFE lens and a plasma-based MFE lens at f = 10 GHz and ν = 1 GHz.

To evaluate the collimating capability of the analytically designed plasma MFE lens, Fig. 3 presents a snapshot of the propagating wave through this lens. This result is obtained by numerically solving the Eikonal equations at a frequency of f = 10 GHz for the refractive index profile shown in Fig. 2. The figure clearly illustrates that the beam is collimated after passing through the plasma MFE lens. In this simulation, the feed is a rectangular waveguide (WR90).

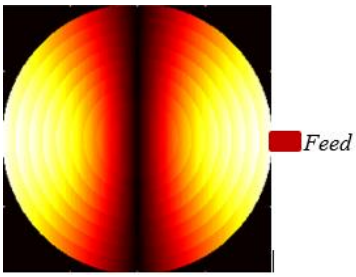

Fig. 3. Snapshot showing the analytically obtained propagating wave from the plasma MFE lens at f = 10 GHz corresponding to the refractive index profile illustrated in Fig. 2.

In the following section, the performance and feasibility of the proposed plasma MFE lens are further analyzed through full-wave electromagnetic computations.

4. DESIGN OF A PROTOTYPE AND NUMERICAL INVESTIGATION

In this section, a plasma-based MFE lens antenna is designed based on the analytical equations presented in the previous section for operation at f = 10 GHz. The performance of the designed lens is evaluated through numerical simulations, considering two configurations: a spherical lens and a hemispherical lens.

For simulation purposes, the time-domain solver of the commercial software CST Microwave Studio® is employed. Moreover, a rectangular waveguide (WR90) is placed in front of the lens to illuminate the lens. For an MFE lens, a waveguide feed offers advantages in terms of integration and compactness, particularly at higher frequencies. However, the type of feed does not significantly affect the overall performance of the lens and thus can be replaced with other feeds such as horn antennas.

Let's start with the design of the spherical MFE plasma lens which has a radius of R = 100 mm. The plasma medium is modelled as collisional, with a collision frequency of ν = 1 GHz, to provide a more realistic representation of the lens's performance. Based on these initial parameters, plasma frequency distribution is derived, as shown by the red dashed line in Fig. 4.

It's important to note that in practical applications, a stepped index profile is typically used to implement MFE lenses. Accordingly, in this study, the plasma frequency distribution is discretized along the lens radius, forming a staircase-like profile, as shown by the solid black line in Fig. 4. So, the plasma MFE lens, as depicted in Fig. 6, is divided into ten distinct spherical layers, each with a thickness of 10 mm.

To calculate the characteristics of the various layers, with each outer radius denoted by r_i (where i represents the layer number from 1 to 10), the following procedure is employed:

- An initial refractive index of n_0 = 1 is assumed at the center of the sphere.
- The refractive index $n_p(r_i)$ for each layer is calculated using Eq. (5), with results displayed in Fig. 6, comparing the continuous inhomogeneous and stepped index profiles.
- Finally, the plasma frequency for each layer, $f_p(r_i)$, is computed using Eq. (12).

Note that for simplicity, the impact of dielectric containers surrounding the spherical layers has been neglected in this feasibility study. Following the procedure, the characteristics of the plasma MFE lens are determined. In practice, a controllable DC

power supply based on an electrical dimmer can effectively adjust the plasma frequency in the layers. For instance, in [17], the plasma frequency was controllable between 2 GHz and 7.8 GHz using DC biasing. This flexibility allows for fine-tuning the refractive index of plasma, enabling dynamic control of the properties of the lens. While this method has successfully stabilized plasma states, alternative methods, such as AC or pulsed biasing, may further enhance flexibility, providing additional options for optimizing plasma performance in this application.

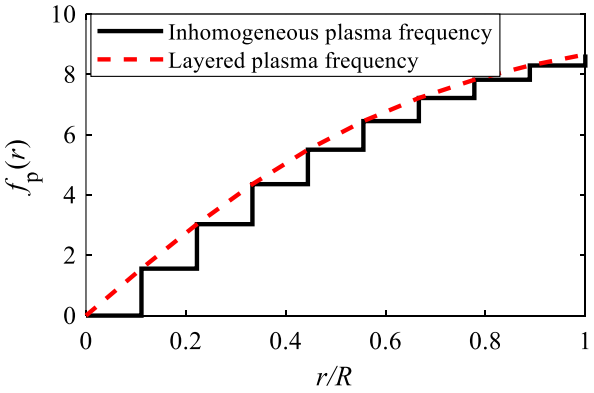

Fig. 4. Plasma frequency versus normalized radius of the plasma MFE lens.

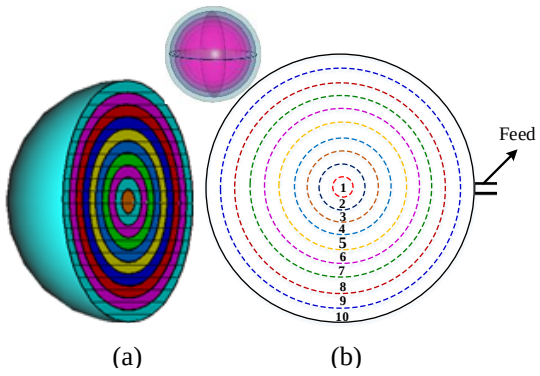

Fig. 5. (a) 3-D view, (b) side view of the ten-layer plasma MFE lens.

Table 1. Permittivity of the plasma layers in the plasma MFE lens.

Parameter	Quantity
$\varepsilon_p(r_{10})$	0.25
$\varepsilon_p(r_9)$	0.31
$\varepsilon_p(r_8)$	0.38
$\varepsilon_p(r_7)$	0.47
$\varepsilon_p(r_6)$	0.58
$\varepsilon_p(r_5)$	0.69
$\varepsilon_p(r_4)$	0.81
$\varepsilon_p(r_3)$	0.9
$\varepsilon_p(r_2)$	0.97
$\varepsilon_p(r_1)$	1

A snapshot of the magnitude of the computed electric field before and after passing through the lens is illustrated in Fig. 7. Similar to Fig. 3, this figure demonstrates the collimation of the beam after passing through the lens. Due to the reconfigurable nature of plasma, exciting the spherical MFE plasma lens increases the gain of the feed by approximately 6.5 dB, as illustrated in Fig. 8, while deactivating the lens cancels the focusing effect.

In summary, it is observed that using plasma dielectrics, a reconfigurable spherical MFE lens can be realized, although the distribution of the dielectric permittivity in the lens structure differs from conventional MFE lenses. In other words, the permittivity decreases from close to 1 at the center to 0.25 at the outer layer of the lens. Despite the significant difference in the values of refractive index or permittivity, a plasma-based MFE lens, similar to conventional MFE lenses, focuses on the radiated beam of the feed antenna.

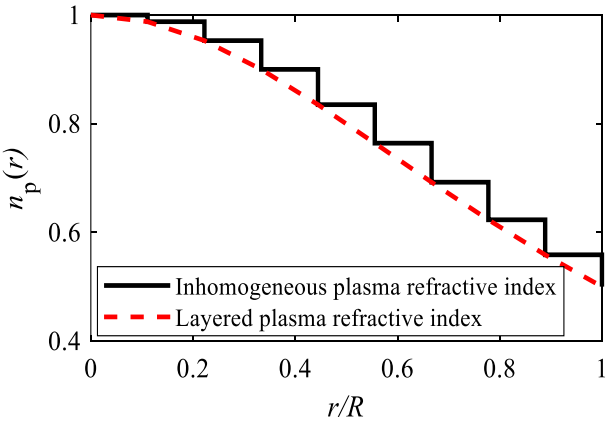

Fig. 6. Refractive index versus normalized radius of the plasma MFE lens.

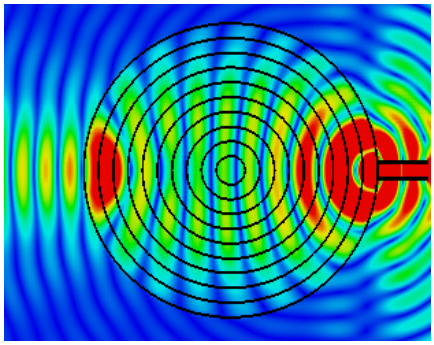

Fig. 7. Snapshot of numerical E-field distribution of the plasma MFE lens at f = 10 GHz.

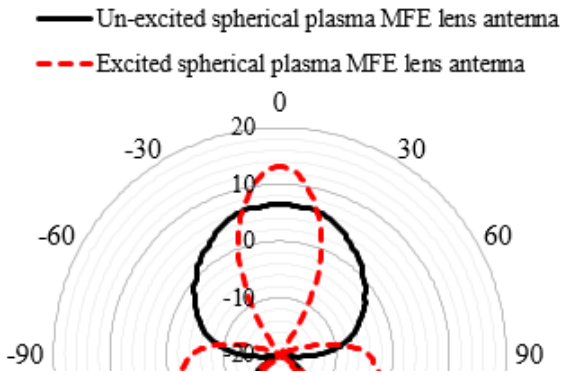

Fig. 8. Simulated gain of the spherical plasma MFE lens antenna at f = 10 GHz.

Now let us continue this section with a hemispherical plasma MFE lens. The structure comprises the waveguide feed, integrated with half of the ten-layer plasma-based spherical MFE lens designed in the previous step. The magnitude of the electric field before and after passing through the excited lens antenna, at the operating frequency of f = 10 GHz, is depicted in Fig. 9(a). Notably, by activating the plasma, the incident spherical wave transforms into a plane wave upon passing through the lens. Additionally, Fig. 9(b) presents a 3-D view of the simulated radiation pattern of this lens antenna.

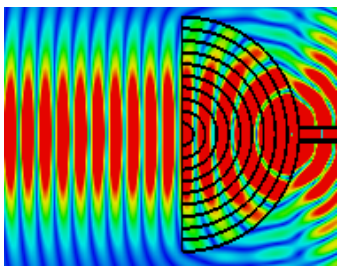

(a)

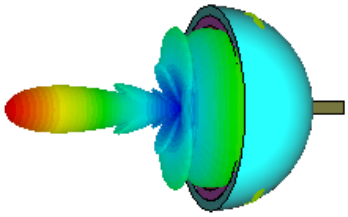

(b)

Fig. 9. (a) Magnitude of the electric field at 10 GHz before and after passing the hemispherical MFE plasma lens, (b) A 3-D view of the simulated radiation pattern of the hemispherical MFE plasma lens antenna.

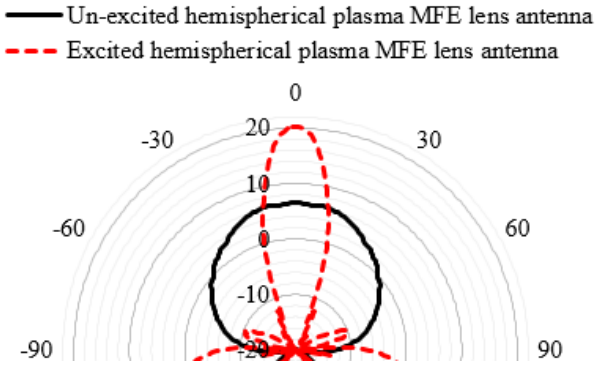

Fig. 10. Simulated gain of the hemispherical plasma MFE lens antenna at f = 10 GHz.

The simulation results reveal a gain of approximately 19.9 dBi with a half-power beamwidth (HPBW) of around 12 degrees for the lens antenna. Moreover, the proposed lens exhibits a 12.8 dBi enhancement in gain, focusing the beam effectively, as demonstrated in Fig. 10. When the plasma is deactivated, the gain of the antenna structure decreases to that of the gain of the feed. Hence, the lens antenna proves to be reconfigurable, possessing the capability to regulate radiation gain and, consequently, the beamwidth.

5. PARAMETRIC ANALYSIS

In this section, numerical simulations are conducted to evaluate the impact of varying the plasma bias characteristics on the performance of the proposed MFE lens. Furthermore, the effect of layer thickness within the lens is analyzed to determine the optimal number of layers for a constant lens radius.

First, we consider the ten-layer hemispherical plasma MFE lens designed in the previous section as the baseline antenna. The goal is to assess how

deactivating certain plasma layers affects the radiation characteristics, as the plasma layers can be independently switched ON or OFF. Concerning the layer numbering in Fig. 5(b), Fig. 11 illustrates that deactivating the inner layers leads to a reduction in radiation gain. For example, when all plasma layers are OFF, the antenna gain is 8 dBi. Activating only layer 10 increases the gain to 12.2 dBi, and further enhancement to 13.6 dBi is achieved when both layers 9 and 10 are ON. When all plasma layers are ON, the antenna achieves a maximum gain of around 19.9 dBi.

This demonstrates the ability to dynamically control the radiation characteristics by adjusting the bias of individual lens layers.

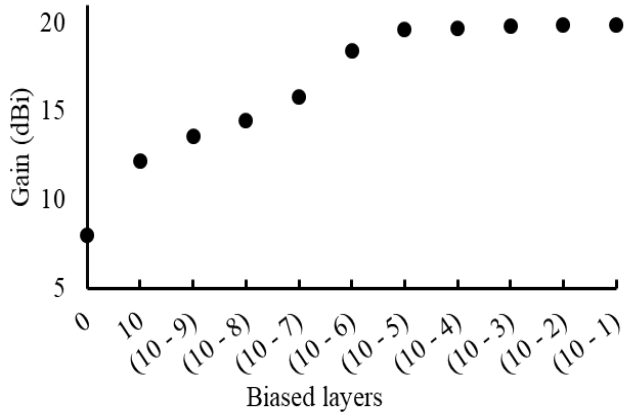

Fig. 11. Radiation gain as a function of the number of excited layers in the lens.

In the next step, the effect of layer thickness on the antenna's radiation characteristics is examined. It is evident that increasing the number of layers makes the lens behavior more like that of a truly inhomogeneous lens. However, reducing the number of layers simplifies the implementation. Therefore, a compromise must be made between optimizing radiation performance and minimizing implementation complexity.

As shown in Fig. 12, reducing the thickness of the layers increases the radiation gain. However, for thicknesses of $t = 5$ mm and $t = 10$ mm, the radiation gains are nearly identical. Therefore, selecting $t = 10$ mm can be considered the optimal layer thickness, offering a good compromise between performance and practicality.

In summary, the parametric analysis demonstrates that by controlling the plasma layers one can dynamically adjust the gain, with an optimal layer thickness of $t = R/10$ providing the best trade-off between gain and implementation simplicity.

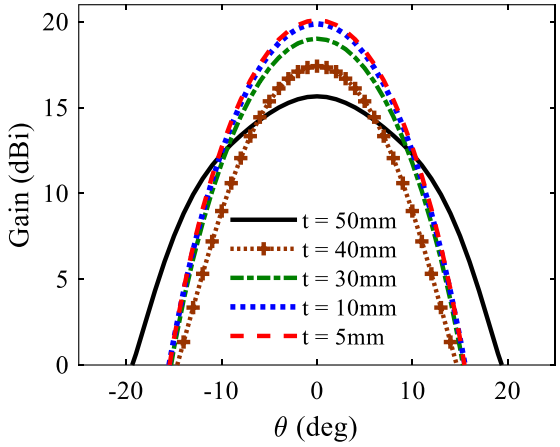

Fig. 12. Radiation gain of the lens antenna for various layer thicknesses in the plasma MFE lens.

6. CONCLUSION

This study investigated the feasibility and performance of utilizing plasma dielectric material within Maxwell Fish Eye (MFE) lens antenna structures for achieving reconfigurability. Through numerical simulations, it was demonstrated that plasma-based MFE lens antennas offer promising capabilities in dynamically tailoring radiation patterns and beam directions.

The unique refractive index profile of plasma dielectrics and their impact on MFE lens design and performance were highlighted. By incorporating plasma dielectric material, reconfigurable lens antennas capable of enhancing beam focusing and gain were shown to be feasible.

CONFLICT OF INTERESTS

No conflict of interest has been expressed by the authors.

REFERENCES

[1] L. Gunderson, "An electromagnetic analysis of a cylindrical homogeneous lens," *IEEE Transactions on Antennas and Propagation*, vol. 20, no. 4, pp. 476-479, 1972, https://doi.org/10.1109/TAP.1972.1140224.

[2] J. Liu, R. Mendis, and D. M. Mittleman, "A 2D Maxwell's fish eye lens using waveguide-based inhomogeneous artificial dielectrics," in *CLEO: 2013*, San Jose, California, USA, 2013, Art. no. CTh1k.3, Optica Publishing Group, https://doi.org/10.1364/CLEO_SI.2013.CTh1K.3.

[3] D. H. Werner, Z. Jiang, J. P. Turpin, and P. L. Werner, "Transformation optics collimating lenses for multi-beam antenna applications," in *4th IEEE International Symposium on Microwave, Antenna, Propagation and EMC Technologies for Wireless Communications*, Beijing, China, 2011, pp. 458-461, https://doi.org/10.1109/MAPE.2011.6156192.

[4] F. E. Helmy, I. I. Ibrahim, and A. M. Saleh, "Beam-steering of dielectric flat lens nanoantenna with elliptical patch based on antenna displacement for optical wireless applications," *Scientific Reports*, vol. 13, 2023, Art. no. 16030, https://doi.org/10.1038/s41598-023-43149-z.

[5] M. M. Taskhiri and S. Fakhte, "Broadband inhomogeneous lens with conical radiation pattern," *Scientific Reports*, vol. 13, 2023, Art. no. 12907, https://doi.org/10.1038/s41598-023-40024-9.

[6] H. F. Ma, B. G. Cai, T. X. Zhang, Y. Yang, W. X. Jiang, and T. J. Cui, "Three-dimensional gradient-index materials and their applications in microwave lens antennas," *IEEE Transactions on Antennas and Propagation*, vol. 61, no. 5, pp. 2561-2569, 2013, https://doi.org/10.1109/TAP.2012.2237534.

[7] J. Bor, B. Fuchs, O. Lafond, and M. Himdi, "Flat foam-based Mikaelian lens antenna for millimeter wave applications," in *44th European Microwave Conference*, Rome, Italy, 2014, pp. 1640-1643, https://doi.org/10.1109/EuMC.2014.6986768.

[8] B. Fuchs, O. Lafond, S. Rondineau, and M. Himdi, "Design and characterization of half Maxwell fish-eye lens antennas in millimeter waves," *IEEE Transactions on Microwave Theory and Techniques*, vol. 54, no. 6, pp. 2292-2300, 2006, https://doi.org/10.1109/TMTT.2006.875255.

[9] M. A. B. Abbasi, R. I. Ansari, G. G. Machado, and V. F. Fusco, "Design and analysis of Maxwell fisheye lens based beamformer," *Scientific Reports*, vol. 11, 2021, Art. no. 22739, https://doi.org/10.1038/s41598-021-02058-9.

[10] H. Lu, G. Wu, Y. Liu, and X. Lv, "A millimeter-wave fully metallic six-channel crossover based on Maxwell fish-eye lens," *IEEE Microwave and Wireless Components Letters*, vol. 30, no. 11, pp. 1041-1044, 2020, https://doi.org/10.1109/LMWC.2020.3027466.

[11] Q. Lei, R. Foster, P. S. Grant, and C. Grovenor, "Generalized Maxwell fish-eye lens as a beam splitter: A case study in realizing all-dielectric devices from transformation electromagnetics," *IEEE Transactions on Microwave Theory and Techniques*, vol. 65, no. 12, pp. 4823-4835, 2017, https://doi.org/10.1109/TMTT.2017.2727495.

[12] N. Muhamad Nadzir, M. Himdi, M. K. A. Rahim, N. A. Murad, O. Ayop, and O. Lafond, "Multi-beam luneburg lens with reduced size patch antenna," *Electronics*, vol. 12, no. 14, 32023, Art. no. 3028, https://doi.org/10.3390/electronics12143028.

[13] Y. Shi, K. Li, J. Wang, L. Li, and C. H. Liang, "An etched planar metasurface half Maxwell fish-eye lens antenna," *IEEE Transactions on Antennas and Propagation*, vol. 63, no. 8, pp. 3742-3747, 2015, https://doi.org/10.1109/TAP.2015.2438337.

[14] H. Lu, Z. Liu, Y. Zhang, K. Pang, and Y. Liu, "Partial Maxwell fish-eye lens inspired by the Gutman lens and Eaton lens for wide-angle beam scanning," *Optics Express*, vol. 29, no. 15, pp. 24194-24209, 2021, https://doi.org/10.1364/OE.426539.

[15] T. Tandel and S. Trapasiya, "Reconfigurable antenna for wireless communication: Recent developments, challenges and future," *Wireless Personal Communications*, vol. 133, no. 2, pp. 725-768, 2023, https://doi.org/10.1007/s11277-023-10785-7.

[16] S. Dubal and A. Chaudhari, "Mechanisms of reconfigurable antenna: A review," in *10th International Conference on Cloud Computing, Data Science & Engineering (Confluence)*, Noida, India, 2020, pp. 576-580, https://doi.org/10.1109/Confluence47617.2020.9057998.

[17] F. Sadeghikia, K. Zafari, M. R. Dorbin, M. Himdi, and A. K. Horestani, "Reconfigurable biconcave lens antenna based on plasma technology," *Scientific Reports*, vol. 13, 2023, Art. no. 9213, https://doi.org/10.1038/s41598-023-36332-9.

[18] M. O. Arend, F. C. C. D. Castro, C. Müller, and M. C. F. D. Castro, "Toroidal plasma lens antenna," *IEEE Antennas and Wireless Propagation Letters*, vol. 16, pp. 1155–1158, 2016, https://doi.org/10.1109/LAWP.2016.2625800.

[19] F. Sadeghikia, K. Zafari, M. Himdi, M. T. Noghani, and A. K. Horestani, "An advanced beamforming mechanism based on programmable plasma prisms," *IEEE Access*, vol. 12, pp. 182062-182072 2024, https://doi.org/10.1109/ACCESS.2024.3506821.

[20] H. Ja'afar, M. T. B. Ali, A. N. B. Dagang, H. M. Zali, and N. A. Halili, "A reconfigurable monopole antenna with fluorescent tubes using plasma windowing concepts for 4.9-GHz

application," *IEEE Transactions on Plasma Science*, vol. 43, no. 3, pp. 815-820, 2015, https://doi.org/10.1109/TPS.2015.2398878.

[21] F. Sadeghikia, M. Valipour, A. K. Horestani, M. Himdi, and T. Anderson, "Beam-steerable helical antenna using plasma reflectors," in *16th European Conference on Antennas and Propagation (EuCAP)*, Madrid, Spain, 2022, https://doi.org/10.23919/EuCAP53622.2022.9769604.

[22] F. Sadeghikia, A. K. Horestani, and M. Himdi, "Reconfigurable antennas based on plasma reflectors and cylindrical slotted waveguide," in *Plasma Science-Recent Advances, New Perspectives and Applications*, S. Singh. Ed. London, United Kingdom: IntechOpen, 2022, https://doi.org/10.5772/intechopen.108017.

[23] F. Sadeghikia, M. R. Dorbin, A. K. Horestani, M. T. Noghani, and H. Ja'afar, "Tunable inverted-F antenna using plasma technologies," *IEEE Antennas and Wireless Propagation Letters*, vol. 18, no. 4, pp. 702-706, 2019, https://doi.org/10.1109/LAWP.2019.2901354.

[24] J. Bazrafshan, F. Sadeghikia, A. K. Horestani, and M. Himdi, "A reconfigurable and steerable horn antenna using plasma dielectric slabs for controllable gain and beam steering," *Journal of Space Science and Technology*, vol. 17, no. 3, pp. 28-44, 2024, https://doi.org/10.22034/jsst.2024.1455.

[25] T. Anderson, "Antenna beam focusing and steering with refraction through a plasma," in *13th European Conference on Antennas and Propagation (EuCAP)*, Krakow, Poland, 2019, pp. 1-5.

[26] F. Sadeghikia, M. Valipour, M. T. Noghani, H. Ja'afar, and A. K. Horestani, "3D beam steering end-fire helical antenna with beamwidth control using plasma reflectors," *IEEE Transactions on Antennas and Propagation*, vol. 69, no. 5, pp. 2507–2512, https://doi.org/10.1109/TAP.2020.3031473.

[27] A. K. Horestani, M. T. Noghani, F. Sadeghikia, M. R. Dorbin, M. Valipour, and F. Martín, "Reconfigurable and frequency tunable inverted F antenna based on plasma technology," in *International Conference on Electromagnetics in Advanced Applications (ICEAA)*, Granada, Spain, 2019, pp. 1175-1177, https://doi.org/10.1109/ICEAA.2019.8879280.

[28] M. R. Dorbin, J. A. R. Mohassel, F. Sadeghikia, and H. B. Ja'afar, "Determination of the plasma density in a plasma antenna based on image analysis and LIVPD graphs," *IEEE Access*, vol. 11, pp. 120721-120727, 2023, https://doi.org/10.1109/ACCESS.2023.3327179.

[29] F. Sadeghikia and F. Hodjat Kashani, "A two element plasma antenna array," *Engineering, Technology and Applied Science Research*, vol. 3, no. 5, pp. 516–521, 2013, https://doi.org/10.48084/etasr.319.

[30] M. T. Noghani, A. K. Horestani, F. Sadeghikia, and M. R. Dorbin, "Theoretical modeling of resonant wavelength in 3-layered plasma antennas," *Waves in Random and Complex Media*, vol. 31, no. 6, pp.1587-1596, 2021, https://doi.org/10.1080/17455030.2019.1687959.

[31] M. Magarotto *et al.*, "Plasma antennas: A comprehensive review," *IEEE Access*, vol. 12, pp. 80468-80490, 2024, https://doi.org/10.1109/ACCESS.2024.3411142.

[32] S. H. Zainud Deen, H. A. E. A. Malhat, E. A. E. Refaey, and M. M. Badawy, "Genus plasma-based self-complementary reconfigurable intelligent metasurfaces," *Plasmonics*, vol. 19, pp. 2991-3001, 2024, https://doi.org/10.1007/s11468-024-02215-6.

[33] F. Sadeghikia, A. K. Horestani, M. R. Dorbin, M. T. Noghani, and H. Ja'afar, "A new feed network for the communication signal and excitation of surface-wave-driven plasma antennas," in *14th European Conference on Antennas and Propagation (EuCAP)*, Copenhagen, Denmark, 2020, pp. 1-4, https://doi.org/10.23919/EuCAP48036.2020.9135951.

[34] F. Sadeghikia, M. R. Doorbin, H. Ja'afar, A. K. Horestani, and M. T. Noghani, "An overview on the implementation of surface wave driven plasma antennas," in *IEEE Symposium on Wireless Technology & Applications (ISWTA)*, Shah Alam, Malaysia, 2021, pp. 53-57, https://doi.org/10.1109/ISWTA52208.2021.9587357.

[35] E. Koohkan, S. Jarchi, A. Ghorbani, and M. Bod, "Vortex beam generation based on plasma reflect-array surface at microwave frequencies," *IEEE Transactions on Plasma Science*, vol. 49, no. 7, pp. 2086-2092, 2021, https://doi.org/10.1109/TPS.2021.3083199.

[36] G. Mansutti, P. D. Carlo, M. Magarotto, M. A. Hannan, P. Rocca, and A. D. Capobianco, "Design of a hybrid metal-plasma transmit-array with beam-scanning capabilities," *IEEE Transactions on Plasma Science*, vol. 50, no. 3, pp. 662-669, 2022, https://doi.org/10.1109/TPS.2022.3149473.

[37] F. Sadeghikia, M. T. Noghani, and M. R. Simard, "Experimental study on the surface wave driven plasma antenna," *AEU-International Journal of Electronics and Communications*, vol. 70, no. 5, pp. 652– 656, 2016, https://doi.org/10.1016/j.aeue.2016.01.024.

[38] M. Born, and E. Wolf, *Principles of Optics: Electromagnetic Theory of Propagation, Interference and Diffraction of Light*, 6th ed. Cambridge University Press, 1980.

[39] D. S. Kulyabov, M. N. Gevorkyan, and A. V. Korolkova, "Software implementation of the Eikonal equation," in *VIII Conference Information and Telecommunication Technologies and Mathematical Modeling of High-Tech Systems*, Moscow, Russia, 2018.